Indonesian Journal of Electrical Engineering and Computer Science
Vol. 24, No. 2, November 2021, pp. 661~672
ISSN: 2502-4752, DOI: 10.11591/ijeecs.v24.i2.pp661-672

High impedance fault detection in 11 kV overhead line with discrete wavelet transform and independent component analysis

Md Ferdouse Hossain Bhuiya[1], Rohaiza Hamdan[2], Dur Mohammad Soomro[3], Abdelrehman Omer Idris[4], Hussain Sharif[5]
[1,2,3]Faculty of Electrical and Electronic Engineering, Universiti Tun Hussein Onn Malaysia, Johor, Malaysia
[4,5]Al Ain Distribution Company, UAE, Department of Electrical Engineering, United Arab Emirates University, Abu Dhabi, United Arab Emirates

Article Info

Article history:

Received Jun 3, 2021
Revised Sep 7, 2021
Accepted Sep 14, 2021

Keywords:

DWT
HIF
ICA
Moving window

ABSTRACT

This paper proposes an analysis of high-impedance fault detection algorithms for medium voltage distribution lines based on the discrete wavelet transform (DWT) technique and a more advanced technique named independent component analysis (ICA) independently. Three-phase distribution line model and two diodes high impedance fault model, which represents the unsymmetrical fault current of electric arc, simulated using MATLAB/Simulink. High impedance fault (HIF) detection algorithm initially analyzes the sampled current waveforms through DWT and the resultant third level high-frequency components "d3" coefficients are analyzed through one cycle moving window approach. The proposed algorithm successfully detects any HIF in the distribution current even if there is a slight or no difference in the amplitude of the HIF and the waveform of the phase current. On the other hand, the ICA more developed algorithm than DWT successfully separated the noise signals from the obtained current waveforms and HIF noise signals can be differentiated with non-HIF noise signals. Because of this reason ICA is chosen in this research. The detected HIF current can be from 50 ma and up.

Corresponding Author:

Rohaiza Hamdan
Department of Electrical and Electronic Engineering
Universiti Tun Hussein Onn Malaysia
86400 Parit Raja, Batu Pahat, Johor, Malaysia
Email: rohaiza@uthm.edu.my

1. INTRODUCTION

Unwanted electrical contact between a bare energized conductor and a non-conductive foreign object is called a high impedance fault (HIF). Non-conductors for materials have a high impedance to the flow of current. Common HIF occurs where conductors are physically damaged and fall onto high impedance surfaces such as asphalt tracks, sand, grass, and trees. These types of defects pose a danger to human life and the environment. Another common form of HIF is a conductor mount system failure, insulation failure or tree branch, vegetation, or wall [1]. The arc signal for these defects is generally the same as the signal for a grounded broken conductor. Also, arcs can occur due to air gaps due to poor contact with floors or grounded objects. For example, Figure 1 illustrates the effects of HIF. This happened in Al Ain, Abu Dhabi, UAE. The 11kV distribution line fell to the ground, but due to the characteristics of the floor, the ground trip relay was not enabled and the feeder was not tripped. At night, when the animals touch the three-phase distribution line, they died. Figure 1 illustrate the effect of HIF, the Camel died due to the fallen wooden pole with live conductors in the ground.

Figure 1. Actual site photo

The majority of HIFs occur at 15 kV and lower distribution voltages, with the problem being worse at lower voltages [2]. If a HIF happens in a distribution system, the fault's high impedance causes little to no variation in the current level when opposed to the load current. This makes traditional over-current relays, especially earth fault relays, difficult to detect. Another distinguishing characteristic of HIFs is their erratic nature, with large and unpredictably fluctuating current levels. As a consequence of arcing, fault signals are also rich in harmonics and have high-frequency components [3], [4]. The essence of HIFs has been a topic of study and analysis since the early 1970s [5] which has resulted in the development of several techniques for HIF detection. The most common detection method is to modify overcurrent protective devices [6], but this design has resulted in several unplanned service interruptions because the electric current level caused by HIFs cannot be distinguished from other non-fault events in the power system. For detecting irregular ground currents, a form of the ground relay was built [7]. However, it has the drawback of being unreliable for highly unbalanced loads and multi-grounded systems.

The principle of intelligent computing (IC) has recently been applied to the detection of HIFs. HIF-generated signals have been discovered to have time-varying characteristics [8]. On this basis, HIFs can be detected using a signal processing technique based on the wavelet transform method [9]. Since it is more effective in tracking time-varying fault signals, this is the technique used in this analysis. Furthermore, when any HIF occurs in a transmission line process, the algorithm built in this study is capable of determining the magnitude of the fault current based on the frequency disturbance [10]. While, using the blind source separation technique, the independent component analysis (ICA) algorithm focused on the IC field to restore the corrupted signal containing uncorrelated noise. As a result, the HIF noise signals can be effectively separated from the phase current waveform. The HIF noise pattern is easily distinguishable from non-HIF noise. Ekici *et al.* suggested an iterative real-time algorithm [11] when they first implemented ICA in the 1980s. The ICA method, on the other hand, was largely unknown until 1994, when it was given a name and implemented as a new idea [12].

The following is the layout of the remainder of this paper: The theoretical history of wavelet transforms as a signal analysis method, as well as the mathematical model of the ICA algorithm, are presented in section 2. After that, section 3 is devoted to modeling and simulations of a high impedance fault on an 11 kV power delivery feeder case study. On the signals produced from the simulations, discrete wavelet analysis and independent component analysis are carried out. Section 4 analyzes the results of each algorithm using frequency analysis and pattern recognition, and section 5 draws the study's conclusion.

2. RESEARCH METHOD

2.1. Discrete wavelet transform (DWT) analysis

The wavelet transform is a recently developed mathematical technique that divides data or a signal into different frequency components in a non-uniform manner, then studies each component with a resolution that is proportional to its scale [13]. Because of its ability to obtain both time and frequency information from transient signals, it is often used in signal analysis. The wavelet transforms (WT) is compared to the fourier transforms (FT) and why the WT is favored over the FT is documented in [14]. The resolution issue of time and frequency remains regardless of the transform used. Multi-resolution analysis (MRA) is another method of signal analysis used to address this. MRA examines the signal at a variety of frequencies and resolutions. It does not resolve all of the signal's spectral components equally [15]. At high frequencies, it is built to achieve good time resolution but poor frequency resolution, and vice versa. This is because signals experienced in practical applications have high-frequency components for short durations and low-frequency components for long durations.

Digital filtering techniques introduced by Mallat in 1988 [16] are used to obtain a time scale representation of a digital signal in DWT. To evaluate the signal at various scales, DWT employs filters with various cut-off frequencies. In (1), the signal is passed through a series of high pass filters to analyze the high frequencies, as well as a series of low pass filters to convolution the signal with the filter's impulse [17].

$$x[n] * h[n] = \sum_{k=-\infty}^{\infty} x[k] * h[n-k] \quad (1)$$

h[n] is the low pass filter impulse, where x[n] is a discrete-time function, n is an integer, and k is an index.

The low-frequency components of many signals are the most important components. It conveys a sign of personality. On the other hand, high-frequency materials do not affect taste. This is the reason for introducing approximation and description in wavelet analysis.

The high-scale, low-frequency components of the signal are approximations, whereas the low-scale, high-frequency components are data. In (2), inner products of the function f(t), the signal and, scale function$\varphi_{j,k}(t)$ with the scaling basis j,k is used to compute approximations (also known as scaling coefficients, $A_{j,k}$).

$$A_{j.k} = \langle f\ (t).\emptyset_{j,k}(t)\rangle = \int_{-\infty}^{\infty} f\ (t)\emptyset_{j,k}\ (t)dt \quad (2)$$

Wavelet coefficients (details) can be calculated from wavelet-based on wavelet, using the inner product of the function f (t) and wavelet function $\psi_{j,k}(t)$:

$$D_{j.k} = \langle f\ (t).\psi_{j,k}(t)\rangle = \int_{-\infty}^{\infty} f\ (t)\psi_{j,k}\ (t)dt \quad (3)$$

Details (also known as wavelet coefficients) are obtained by passing the original signal through a low pass filter, while the original signal is passed through a high pass filter. The inner products of the function f(t) with the wavelet basis, as in the equation, are used to calculate this operation mathematically (3). Where the mother wavelet $\psi(t)$ determines the scale function $\emptyset_{j,k}(t)$ and the wavelet function $\psi_{j,k}\ (t)$ by the following equations [18].

$$\emptyset_{j,k}\ (t) = 2^{j/2}\emptyset(2^j t - k) \quad (4)$$

$$\psi_{j,k}\ (t) = 2^{j/2}\psi(2^j t - k) \quad (5)$$

Unfortunately, if you perform the above operation on a real digital signal, you'll end up with twice as much info. The original signal must be downsampled to correct the problem caused by the filtering operations. Downsampling a signal entails lowering the sampling rate or eliminating any of the signal's samples.

As previously stated, the DWT decomposes signals into coarse approximation and detail and analyzes them at different frequency bands with different resolutions. To accomplish this, DWT employs scaling and wavelet functions. Low pass and high pass filters, respectively, are correlated with these two sets of functions. First, a half-band high pass filter g[n] and a low pass filter h[n] are applied to the initial signal x[n]. As previously said, half of the samples will be discarded after the filtering process. As a result, the signal can be subsampled by two. This is one decomposition level, and it can be expressed mathematically as follows:

$$D_j[n] = \sum_k x[n].g[2n - k] \quad (6)$$

$$A_j[n] = \sum_k x[n].h[2n - k] \quad (7)$$

where Dj is the output of the detailed high pass filter, Aj is the output of the approximate low pass filter, and the resolution j, j = 1,2, ..., J. k = 1,2, ..., K, where K is the length of the filter vector after downsampling to 2 [19]. The signal decomposition method can be repeated by decomposing a continuous approximation one after another by decomposing one signal into several low-resolution components. Figure 2 shows the layout of the DWT. The resolution level has two general meanings. J in descending order from highest resolution level (1) to harshest resolution level (J) and highest resolution level (J1) to most severe resolution level (0). J represents the total resolution level. The relationship between level and j is as follows:

Level = $J - j$

At the bottom of Figure 2, the resolution levels in terms of Level and j are described. Each resolution level's resolution scale, or scale Level, is specified as follows:

$Scale_{\text{Level}} = 2^{J-\text{Level}} = 2^j$

The input signal dj + 1 of the upper-resolution level is divided into approximate cj by the low-pass filter h0 of the upper-resolution level and is divided into the information dj by the high-pass filter h1 at the sub-resolution level of each resolution level. After that, the output approximation and the information signal are reduced by about 2 for both. The maximum frequency of the originally sampled signal f (t) at freqf (t) Hz

is freqf (t) / 2 Hz based on the Nyquist arrangement (the highest frequency that can be correctly represented is less than 1/2. Sampling rate).

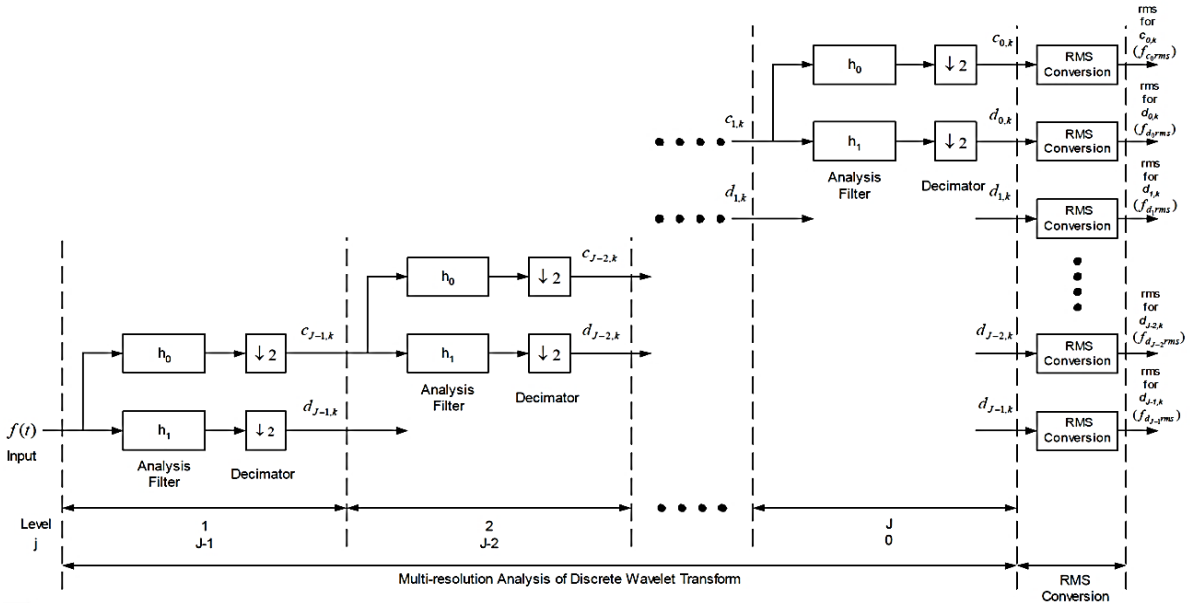

Figure 2. Multiresolution scheme for DWT analysis

2.2. Independent component analysis (ICA)

It is a blind source-based separation approach including an unknown environmental source signal "S" and a mixture of signal "A". The features of ICA contain some dubiety regarding independent components i.e. the determination of component's respective vacancies and order is not possible and hence called a blind source approach. ICA has different typed i.e. Fast ICA, Infomax ICA, and Projection pursuit ICA [20] to extract the independent components considering;

a) Maximization of Non-Guassianity method
b) Minimization of mutual information method
c) Maximum likelihood (ML) estimation method

The ICA used for mix signal; lets the system matrix comprised of two different signals "S1" and "S2" and illustrated mathematically as follow;

$$S = \begin{pmatrix} S1 \\ S2 \end{pmatrix}$$
$$S1 = (S_{11}, S_{12}, S_{13}, \ldots\ldots\ldots\ldots\ldots S_{1N})$$
$$S2 = (S_{21}, S_{22}, S_{23}, \ldots\ldots\ldots\ldots\ldots S_{2N})$$

where "S" is the source signal and "N" represents the number of time-space. The mixture of these signals can be written as;

$$X = AS \tag{8}$$

where "A" represents the coefficient matrix and the derived equation is taken as reference by [21].

In resolution level 1, the first approximation cJ1 and first detail dJ1 are sampled at half of frequency f (t). As a result, In (6) gives the maximum frequencies $freq_{Level}$ of signals cj and dj in each resolution level.

$$freq_{Level} = \frac{freq_S}{2^{Level}} \tag{9}$$

3. MODELING AND SIMULATION

This section comprises the HIF model and the power system model and the DWT-based HIF detection algorithm. HIF model simulates the high impedance fault in the developed power system model and the generated current and voltage waveforms are sampled for the post fault analysis by the proposed DWT algorithm.

3.1. High impedance fault (HIF) model

The simulation uses a simplified 2-diode HIF model [22]. Figure 3(a) shows the circuit of the HIF model. Conversely, the Simulink implementation of this model is shown in Figure 3(b). The arc of sandy soil is the basis of this HIF model. At adjacent points, the model contains two diodes of opposite polarity and two direct current (DC) power supplies Vp and Vn that reflect the starting voltage of the soil and/or the air between the tree and the distribution line. The resilience is denoted by the two resistors Rp and Rn. If the values are not the same, asymmetric fault current simulation is possible. When the phase voltage is greater than the positive DC voltage Vp, the fault current flows towards the ground. If the line voltage is less than the negative DC voltage Vn, the fault current is reversed. As long as the phase voltage is between Vn and Vp, no-fault current flows.

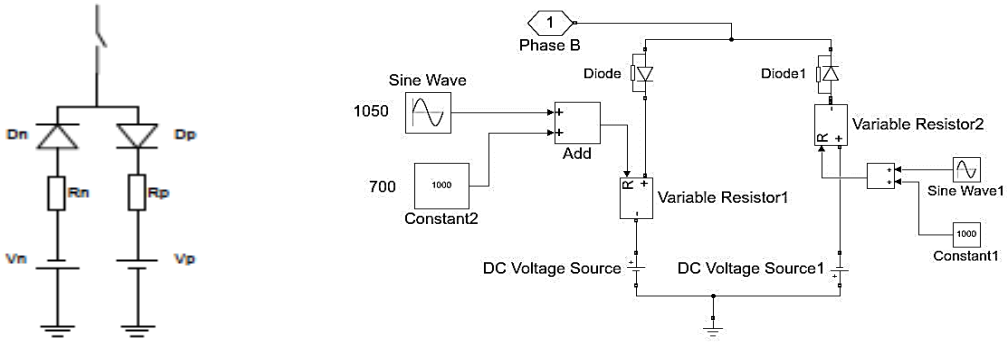

(a) (b)

Figure 3. Simplified two diode HIF fault model; (a) circuit of the HIF model and (b) Simulink implementation

3.2. Power distribution network model

The power distribution network model as illustrated in Figure 4, consists of an 11 kV linear distribution network with two 3 phase Pi section lines, each line is having a length of 25 Km. In the case of the HIF model, variable fault resistance is achieved by introducing a sine wave block with fix 250 Ohm resistance on both branches. Sine wave amplitude is kept at 10% of the fixed resistor value as given in [23].

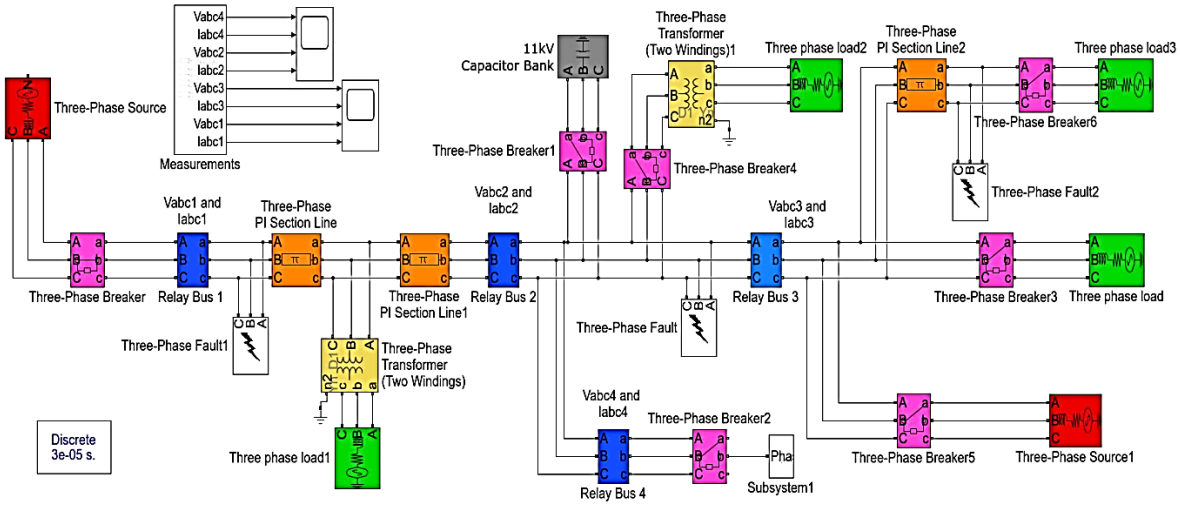

Figure 4. Distribution network model

Furthermore, voltage and current need to be sampled with 256 samples/ cycle so that they can be easily analyzed with DWT and ICA algorithms as well. Specifically, the DWT algorithm accepts 2^n samples for the multiresolution analysis. Therefore sampling time is calculated by using the (10). For the 2 sec simulation time and 50Hz frequency, a total of 25600 samples is generated to be analyzed by the algorithm.

Sample time = (1 cycle period for 50Hz) / (required samples) (10)

3.3. Proposed DWT based HIF detection algorithm

According to the flow chart of Figure 5, this algorithm starts with the separation of each of the 3 current phases Iabc from the combined Iabc to 2D sample array. Afterward, the DWT method provided by MATLAB is applied to each current phase sample and gets d3 coefficient array "d3[n]". Then the next stage is to get the summation of the d3[n]. Since total samples per cycle are set to 256. So that after the 3rd level of DWT, d3 coefficients per cycle are reduced to 256/23 = 32. Therefore, each time 32 coefficients of d3[n] are summed to get sum_d3, which is coefficient summation per electrical cycle. Then Sum_d3 is compared with the threshold value "Th" that has been set to 400 after several iterations. If sum_d3 is equal or above then Th for 7 cycles or more, represented as as "F" variable, this will be the indication of a fault in that specific phase.

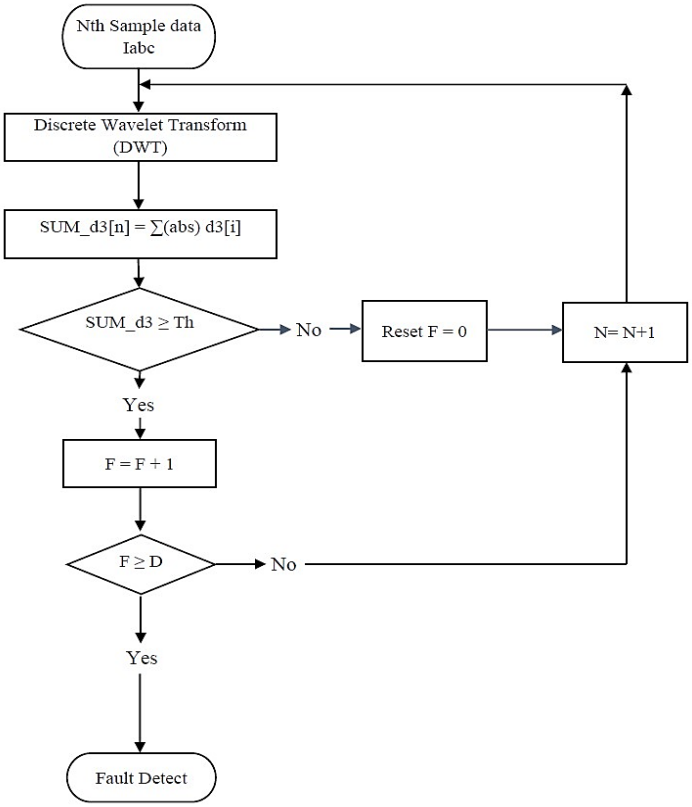

Figure 5. Flow chart of DWT based HIF detection algorithm

3.4. Proposed ICA based HIF detection algorithm

For the ICA algorithm to separate the HIF noise signal from phase current waveforms, it is important to get each phase current sample from at least three different locations because of having three different phases or independent components. According to (8), there should be *n* linear mixtures $x_1,..,x_n$ of *n* independent components $s_{1,}...s_n$. and *a1, a2,. . . an* represents the coefficient matrix [24].

$$x_j = a_1s_1+a_2s_2+...+a_ns_n$$

where $j = 1...n$.

The current measurement block is used at three different locations to capture the three-phase currents. Initially, the proposed ICA-based detection algorithm generates a linear mixture of each phase current and analyzes each mixture individually with ICA, and yields two separate independent components, noise waveform and the original current waveform for each current phase. ICA method or function has been configured after several trials and errors with the following parameters [25].

Approach = deflation
Nonlinearity 'g' = gauss
Finetune = skew
Stabilization = on

Afterward, extracted noise components of each current phase are plotted in the time domain.

4. RESULTS AND DISCUSSIONS

After the development of the HIF simulation model and algorithm scripts for a distribution system based on DWT and ICA, fault conditions have been tested for 2 seconds simulation time. Where high impedance fault was introduced at phase A, from 0.7 s to 1.3s in case of DWT-based fault detection. While in the case of the ICA-based fault noise separation algorithm fault was introduced in phase B from 0.4sec to 0.405 sec. Fault time has been reduced intentionally in the case of ICA algorithm evaluation so that separated HIF noise component patterns can be observed easily.

Initially, for evaluating each algorithm, the fault was set in the HIF model. After then extract the voltage and current data into the MATLAB workspace with a sample time of $3.33x10^{-6}$ sec. Since it is intended to get 6000 samples per cycle to achieve a high-resolution noise signal pattern, therefore sample time is calculated by using (11).

$$\text{Sample time} = (\text{1 cycle period for 50Hz}) / (\text{required samples}) \quad (11)$$
$$= 20x10^{-3}/6000$$
$$=3.33x10^{-6} \text{ sec}$$

For the simulation time of 2 sec, the total number of electrical cycles is 50Hz x 2 = 100 cycle.

Therefore, the total number of samples that are extracted in the MATLAB workspace will be, Total No. of cycles x No. of samples per cycle =100 cycles x 6000 = 600,000 samples.

Afterward extracted voltage and current data is used in the DWT and ICA-based HIF detection script for the detection of HIF faults in the phases according to the mentioned algorithm separately. These two algorithms are independent but used the fault data from the same model.

4.1. DWT algorithm: phase a fault from 0.5s – 0.7s

For evaluating the DWT-based HIF detection algorithm, the fault was created through a circuit breaker in phase A from 0.5 sec to 0.7 sec. Figure 6(a) and 6(b) illustrates the voltage and current waveforms during phase a fault condition. From the figures, disturbance can be observed in the voltage and current waveforms as well after 0.5sec. However, current waveforms are more affected by HIF, therefore these waveforms are preferred for the HIF analysis.

Following the procedure, current waveforms are sampled with 6000 samples per cycle and analyzed using a developed detection algorithm. Figure 7(a) illustrates the current waveform of phase A, while Figure 7(b) is the graph obtained from its d3 coefficients. In this figure, frequency disturbance can be observed for the fault duration. Moreover, Figure 7(c) illustrates the graph obtained by summing the coefficients of DWT level 3 for each electrical cycle. Since according to the detection algorithm, the threshold value of d3 coefficients summation is set to 800, and if d3 coefficient summation maintains or exceeds this threshold value for at least 7 electrical cycles, this will indicate the presence of HIF in that particular phase. It can be observed in this figure that during the whole fault time, the maximum value of d3 coefficients summation reached about 870. Whereas the minimum value is maintained near about 860, which is higher than the minimum threshold value of 800. Hence, the algorithm successfully detected HIF in phase A and the duration of HIF is calculated through initial and final detection time using relations.

Detection time = (time period of electrical cycle) x (n^{th} d3 coefficient summation after detection)

Initial detection time = (1/50) x 35 = 0.7 sec

Final detection time = (1/50) x 65 = 1.3 sec

An n^{th} number of d3 coefficient summation for initial and final detection time can be observed in Figure 7(c) at the beginning and end of the fault waveform. It is noted that the total number of d3 coefficient summations is the same as the total number of the electrical cycle that is 100 for the 2-sec duration of simulation, since each summation is calculated for one electrical cycle as discussed before.

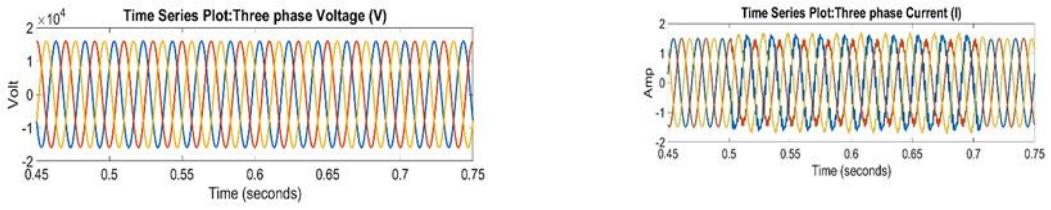

(a) (b)

Figure 6. Voltage and current waveforms for faults in Phase-A condition; (a) voltage and (b) current waveforms

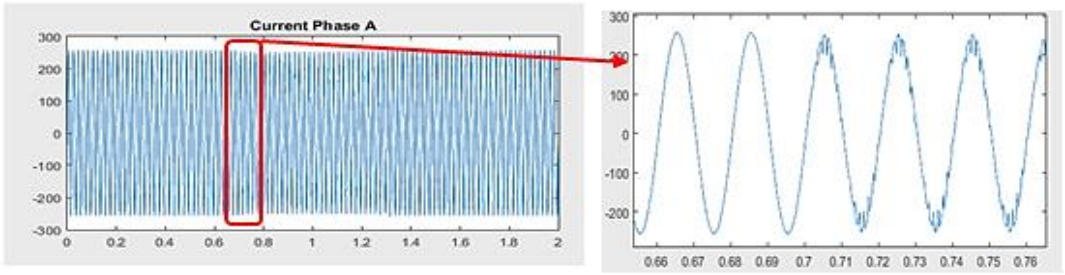

(a)

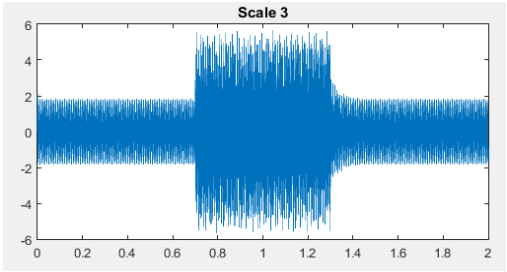

(b) d3A

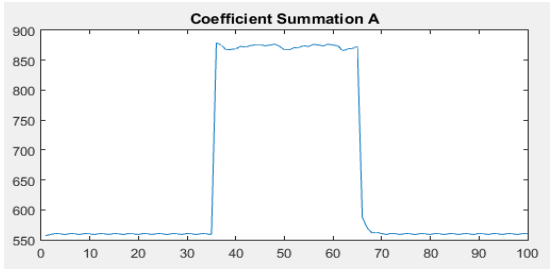

(c) sumD3A

Figure 7. (a) Phase A current (Ia), (b) d3 coefficients of Ia, (c) summation of d3 coefficients of Ia

Meanwhile, Figure 8(a) illustrates the graph obtained from phase B current samples, where as Figure 8(b) represents the graph of d3 coefficients of Ib where minor frequency disturbance can be observed. It is due to the fault in phase A which causes minor disturbance in other phases as well. Figure 8(c) shows the graph of the d3 coefficient summation of Ib. When the DWT algorithm is applied to it. The maximum level of sumd3 coefficients reached 572. Since for HIF detection, at least seven consecutive sum_d3 coefficients should be above the threshold limit of 800, therefore detection algorithm does not detect HIF in phase B in this scenario.

Similarly, Figure 9(a) illustrates the graph obtained from the phase C current (Ic) samples, whereas Figure 9(b) represents the graph of d3 coefficients of Ic, and Figure 9(c) shows the graph of d3 coefficient summation of Ic. Likewise, in the case of Ic, both Figures 9(b) and 9(c) indicate frequency disturbance with the maximum value of sumd3 coefficients reached below the threshold limit of 800. Therefore, the DWT detection algorithm did not detect HIF in phase C because only two coefficients of sum_d3 reached above the threshold limit.

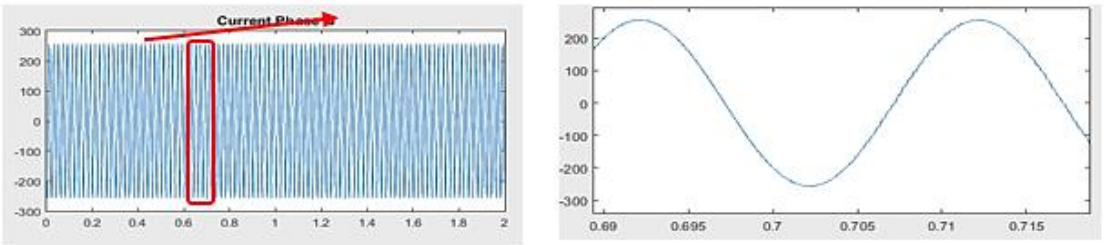

(a)

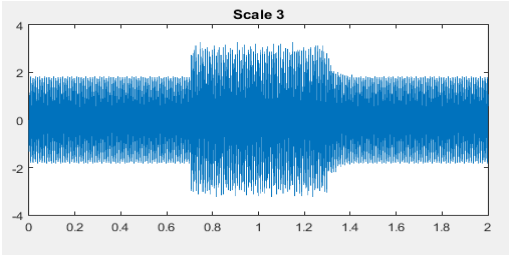

(b)

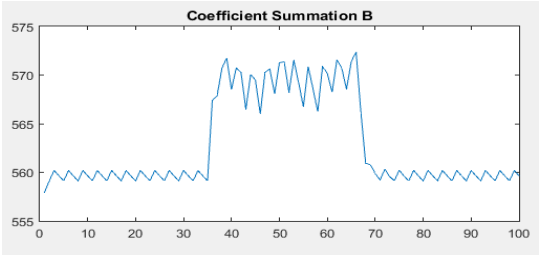

(c)

Figure 8. (a) Phase B current (Ib), (b) d3 coefficients of Ib, (c) summation of d3 coefficients of Ib

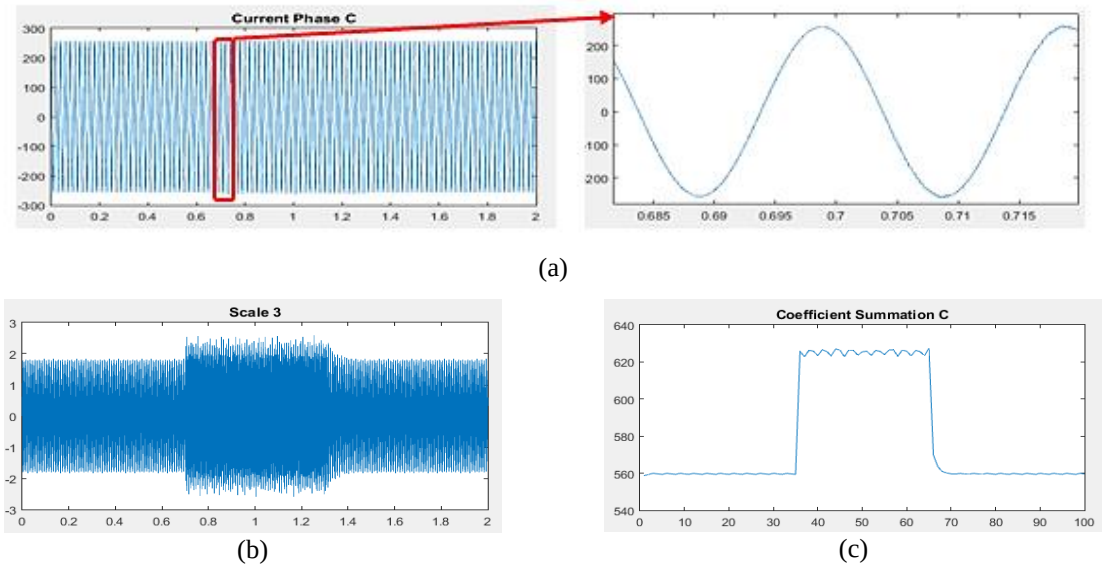

Figure 9. (a) Phase C current, Ic (b) d3 coefficients of Ic, (c) summation of d3 coefficients of Ic

4.2. ICA Algorithm: Phase B Fault from 0.4s – 0.405s

Small noise is created using a Simulink graphical signal generator. This signal was added to the model at phase B in terms of current noise from 0.4 sec to 0.405 sec. To evaluate the developed ICA algorithm feature extraction or noise separation response, Current samples were taken from three different locations of the distribution systems, since the ICA algorithm needs different mixed-signal sources to predict the signal components. Afterward, likewise in the case of the DWT algorithm current waveforms of all the three phases were sampled at 6000 samples/sec and applied the developed ICA algorithm to separate the signal components. Following are the signal components of each phase predicted and separated by the ICA algorithm.

Figure 10 illustrates phase A noise components predicted by the ICA algorithm. Noise pattern is obtained from 0.4 sec to 0.405 sec but it is observed as non-HIF due to its sinusoidal behavior with variable or decreasing amplitudes, whereas HIF noise signals must be non-sinusoidal and should resemble input noise. Meanwhile, Figure 11 illustrates phase B noise components predicted by the ICA algorithm. Noise pattern is obtained from 0.4 sec to 0.405 sec. It is observed as non-sinusoidal, irregular and most importantly it is closely resembling with the input noise added to the system. Thus, the developed ICA algorithm successfully separated the HIF noise from phase B.

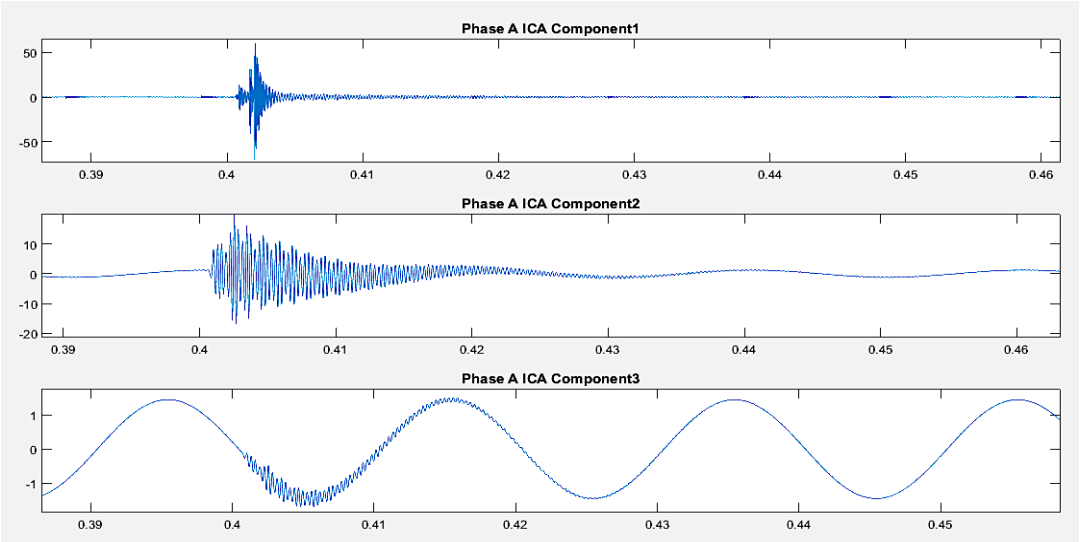

Figure 10. Non-HIF Noise component by ICA algorithm in Phase A

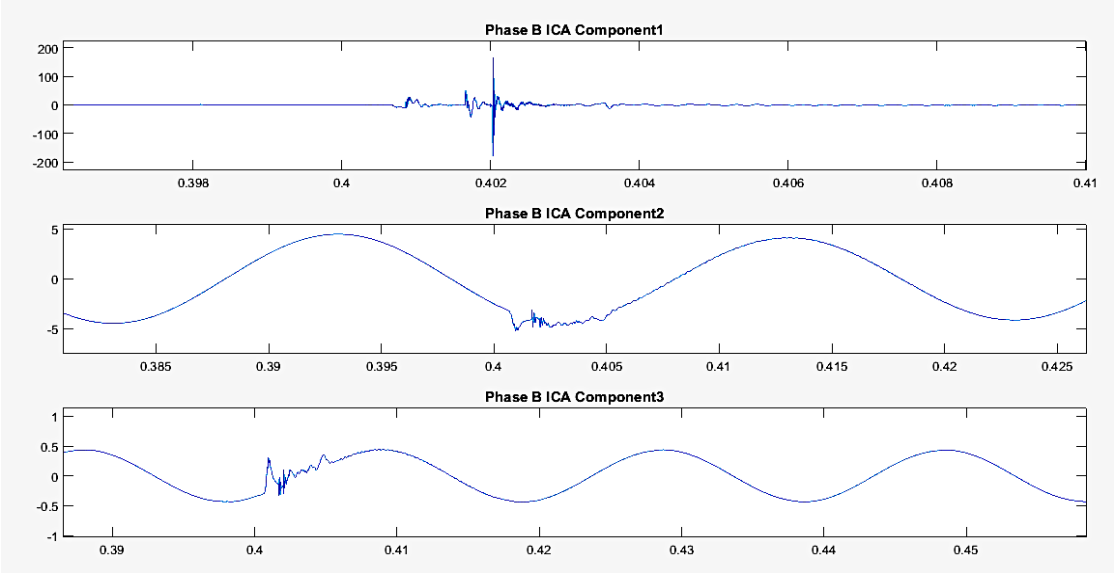

Figure 11. HIF Noise component by ICA algorithm in Phase B

Finally, Figure 12 illustrates the C-phase noise component predicted by the ICA algorithm. The noise mode is obtained from 0.4 seconds to 0.405 seconds, but because its sinusoidal characteristics have variable or reduced amplitude, it is observed as non-HIF, so it can also be observed in the case of phase A. Sine curve, which should be similar to input noise.

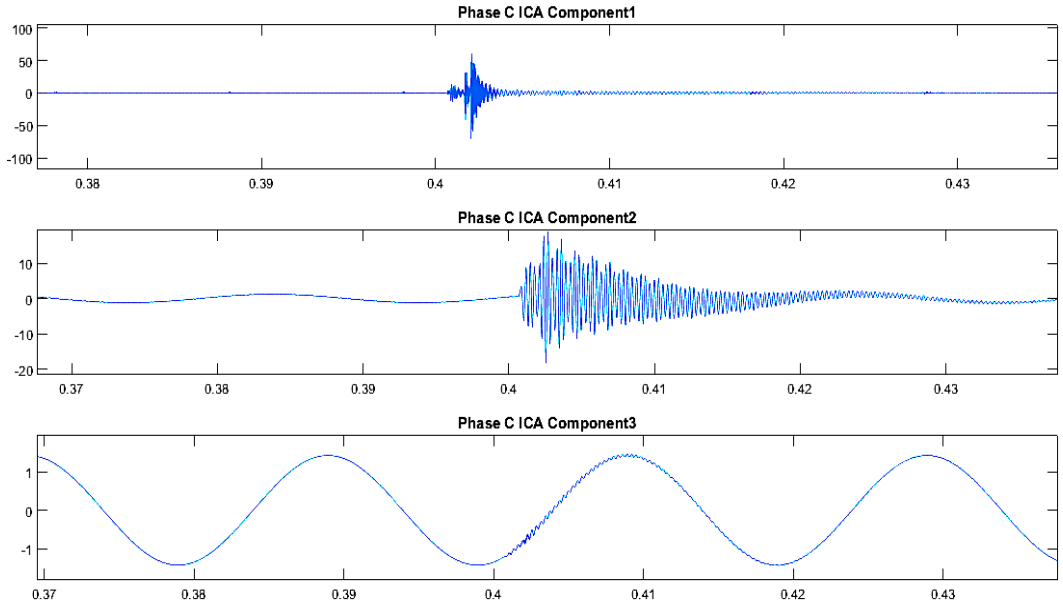

Figure 12. HIF Noise component by ICA algorithm in Phase C

5. CONCLUSION

The main target of this research is to develop DWT and ICA-based algorithms to detect most of the important aspects of HIF characteristics in the current samples generated by the described distribution line simulation. The proposed DWT-based per cycle moving window detection algorithm can precisely predict 90% HIF in the phases at different fault scenarios as demonstrated. However, due to the effect of the faulty phase, minor frequency disturbance was also observed in the non-fault phases. This difficulty is solved by the

algorithm by observing the consistency of frequency disturbance for a certain number of electrical cycles and successfully differentiated between faulty and non-faulty phases. Whereas, the ICA algorithm adopted a different approach in the detection of HIF by taking current samples of each phase from different locations of the distribution line circuit and using the blind source separation technique. Using this technique, 70% of the noise signal could be separated from the phase current, and the algorithm successfully distinguishes HIF noise from non-sinusoidal and irregular, with variable amplitude sinusoidal waveforms, distinguished from non-HIF noise.

REFERENCES

[1] M. Aucoin, "Status of High Impedance Fault Detection," *IEEE Transactions on Power Apparatus and Systems*, vol. PAS-104, no. 3, pp. 637-644, March 1985, doi: 10.1109/TPAS.1985.318999.

[2] Report of PSRC working group D15, "High-impedance Fault Detection Technology," 1996; *retrieved on May 15*, 2009.

[3] J. Stoupis, M. Maharsi, R. Nuqui, S. A. Kunsman, and R. Das, "Reliable Detection of High Impedance Faults Caused by Downed Conductors," *ABB Review*, pp. 1-4, 2004.

[4] B. M. Aucoin, and B. D. Russel, "Distribution High Impedance Fault Detection utilizing High-Frequency Current Components," *IEEE Transactions on Power Apparatus and Systems*, vol. PAS-101, no. 6, pp. 1596-1606, June 1982, doi: 10.1109/TPAS.1982.317209.

[5] J. Stoupis, M. Maharsi, R. Nuqui, S. A. Kunsman, and R. Das, "Ground alert," *ABB review*, vol. 1, pp. 28-31, 2004.

[6] J. Carr, "Detection of High Impedance Faults on Multi-grounded Primary Distribution Systems," *IEEE Transactions on Power Apparatus and Systems*, vol. PAS-100, no. 4, pp. 2008-2016, April 1981, doi: 10.1109/TPAS.1981.316556.

[7] S. Huang and C. Hsieh, "High-impedance Fault Detection Utilizing A Morlet Wavelet Transform Approach," *IEEE Transactions on Power Delivery*, vol. 14, no. 4, pp. 1401-1410, October 1999, doi: 10.1109/61.796234.

[8] R. Polikar, "Fundamental Concepts & an overview of the Wavelet Theory," *Second edition published on*, 2012.

[9] C. H. Kim and R. Aggarwal, "Wavelet Transforms in Power Systems," *Power Engineering Journal*, vol. 14, no. 2, pp. 81-87, April 2000, doi: 10.1049/pe:20000210.

[10] A. Ghaderi, L. Herbert, Ginn III, and H. A. Mohammadpour, "High Impedance Fault Detection: A Review," *Electrical Power System Research*, vol. 143, pp. 376-388, February 2017, doi: 10.1016/j.epsr.2016.10.021.

[11] S. Ekici, S. Yildirim, and M. Poyraz, "Energy and entropy-based feature extraction for locating fault on transmission lines by using neural network and wavelet packet decomposition," *Expert Syst. Appl*., vol. 34, no. 4, pp. 2937-2944, May 2008, doi: 10.1016/j.eswa.2007.05.011.

[12] I. T. Jolliffe, "Principal Component Analysis," *Springer*, New York, 2002.

[13] A. D. Back and A. S. Weigend, "The first application of independent component analysis to extracting structure from stock returns," *Int. J. on Neural Systems*, vol. 8, no. 4, pp. 473-484, 1998, doi: 10.1142/S0129065797000458.

[14] P. Comon, "Independent component analysis - a new concept," *Signal Processing*, vol. 36, pp. 287-314, 1994, doi: 10.1016/0165-1684(94)90029-9.

[15] F. Ferdowsi, H. Vahedi, and C. S. Edrington, "High impedance fault detection utilizing real-time complexity measurement," *2017 IEEE Texas Power and Energy Conference (TPEC)*, 2017, pp. 1-5, doi: 10.1109/TPEC.2017.7868289.

[16] V. C. Nikolaidis, A. D. Patsidis, and A. M. Tsimtsios, "High impedance fault modelling and application of detection techniques with EMTP-RV," *The 14th International Conference on Developments in Power System Protection*, May 2018, doi: 10.1049foe.2018.0217.

[17] T. Cui, X. Dong, Z. Bo, A. Klimek, and A. Edwards, "Modeling Study for High Impedance Fault Detection in MV Distribution System," *International Universities Power Engineering Conference (UPEC)*, 1-4 Sept. 2008, doi: 10.1109/UPEC.2008.4651507.

[18] R. Polikar, "The Wavelet Tutorial," 1994, Retrieved on April 14, 2008.

[19] J. Katende and M. F. Akorede, "Wavelet Transform Based Algorithm for High-Impedance Faults Detection in Distribution Feeders," *European Journal of Scientific Research*, vol. 41, no. 2, pp. 237-247, March 2010.

[20] A. Hyvärinen and E. Oja, "Independent component analysis: algorithms and applications," *Neural networks*, vol. 13, no. 4-5, pp. 411-430, June 2000, doi: doi.org/10.1016/S0893-6080(00)00026-5.

[21] H. C. Dubeya, S. R. Mohanty, N. Kishor, and P. K. Ray, "Fault detection in a series compensated transmission line using discrete wavelet transform and independent component analysis: A comparative study," *2011 5th International Power Engineering and Optimization Conference*, June 2011, pp. 22-26, doi: 10.1109/PEOCO.2011.5970418.

[22] T. M. Lai, L. A. Snider, and E. Lo, "Wavelet Transform Based Relay Algorithm for the Detection of Stochastic High Impedance Faults," *Electric Power Systems Research*, vol. 76, no. 8, pp. 626-633, 2006, doi: 10.1016/j.epsr.2005.12.021.

[23] M. Vetterli and J. Kovačević, "Wavelets and subband coding," *Prentice Hall-PTR Englewood Cliffs, New Jersey*, pp. 1-488, 1995.

[24] A. E. Emanuel, D. Cyganski, J. A. Orr, S. Shiller, and E. M. Gulachenski, "High impedance fault arcing on sandy soil in 15 kV distribution feeders," *Contributions to the evaluation of the low-frequency spectrum*, IEEE Trans. Power Delivery, vol. 5, no. 2, pp. 676-686, April 1990, doi: 10.1109/61.53070.

[25] K. Nikita and P. Khatri, "Analysis and Modeling of High Impedance Fault," *International Journal of Electrical and Electronics Engineering*, vol. 2 no. 3, 2015, doi: 10.14445/23488379/IJEEE-V2I3P101.

BIOGRAPHIES OF AUTHORS

Md Ferdouse Hossain Bhuiya is a student of a fully research-based Masters in Electrical Engineering. Faculty of Electrical and Electronic Engineering in the Universiti Tun Hussein Onn Malaysia (UTHM). He received his Bachelor's degree from Chittagong Univerisity of Engineering and Technology (CUET) in 1996. His research interests include power engineering, control system, and power distribution systems.

Rohaiza Hamdan had joined Universiti Tun Hussien Onn Malaysia (UTHM) as an Academic Staff for more than 15 years and counting. She was graduated from Universiti Tenaga Nasional (UNITEN) and Universiti Teknologi Malaysia (UTM) for Bachelor and Master Programme respectively, both majoring in Electrical Power Engineering. Currently, her research interest encompasses the current advancement in renewable energy, power system stability, and advanced controller development.

Dur Muhammad Soomro is an Assoc. Prof in the field of electrical power engineering. He achieved his bachelor's and masters degrees in 1990 and 2002 respectively from Mehran University of Engineering and Technology (MUET), Jamshoro, Sindh, Pakistan. He was awarded PhD degree in 2011 from Universit Teknologi Malaysia (UTM). His areas of research include power system stability, reliability, protection, quality, distributed generation, and renewable energy.

Abdelrahman Omer Idris currently works with AL Ain Distribution company as a senior control engineer. Received the M.sc Degree in electrical engineering from Dontesk polytechnical Institute in Russian 1992. From 1993 to 1998 work with the Sudan national electricity corporation as an electrical engineer, from 1999 to 2003 work with Sharjah electricity & water authority as a distribution electrical engineer, from 2004 up to now work with Al Ain Distribution Company, in 2015 received Phd degree from UTM, Malaysia. His research interest includes power system and distribution system operation, power quality renewable energy, and power system automation.

Hussain Shareef (Member, IEEE) received his B.Sc. degree (Hons.) from IIT, Dhaka, Bangladesh, M.S. degree from METU, Turkey, and Ph.D. degree from UTM, Malaysia, in 1999, 2002, and 2007, respectively. He is currently a professor in the department of electrical engineering, United Arab Emirates University. His current research interests are power system optimization, power quality, artificial intelligence, renewable energy, and power system automation.